ANL-TRANS-956

ARGONNE NATIONAL LABORATORY
Argonne, Illinois

RF LOSSES IN SUPERCONDUCTING HELIX RESONATORS (≈100 MHz RANGE) CAUSED BY FROZEN-IN MAGNETIC FIELD

(Hochfrequenzverluste in Sl-Wendelresonatoren (100 MHz-Bereich) verursacht durch Eingefrorenes Magnetfeld

by

B. Piosczyk

Report
Source: IEKP II/III. Interner Bericht 73-3-LIN. May 1973. Kernforschungszentrum Karlsruhe. Institut für Experimentelle Kernphysik

Translated from German
by
Arthur H. Jaffey
July 1974

MASTER

I. INTRODUCTION

The measurements described here were carried out in connection with research on the surface resistance in superconducting rf-resonators. Although a few measurements exist in the GHz-range covering the losses caused by frozen-in field[1,2,3], in the 100-MHz region there are only a few measurements and then only at small rf-field intensities [5,6,7]. Since for application in accelerators, the resonators are operated at high field strength, it is of practical interest to know the losses due to frozen-in fields at large rf-field strengths as well.

Because of the relatively complex form of helix resonators, thermally-induced currents may arise during cooldown.[8] In addition, an external magnetic field (e.g. earth's field) may be frozen-in during the transition to superconductivity, leading to increased losses. The losses due to frozen-in field can be a non-negligible part of the so-called residual resistance of a s.c. - resonator, for which other mechanisms are still unclear. In order to identify losses due to frozen-in field in the helix resonator, the corresponding surface resistance R_H was systematically investigated as a function of temperature T, the rf field H_p, and the frequency f. In addition complementary measurements by P. Kneisel and O. Stoltz[4] were carried out on S-band resonators.

II. MEASUREMENT APPARATUS AND PROCEDURES

Measurements were made on two different helix resonators (Fig. 1) of pure Nb. The measuring apparatus is described in Ref. 9. For the first helix resonator (Helix I), the helix was wound of 6.3 x 0.75 mm Nb tubing and welded to the Nb outer tank. The lower cover of the outer tank was (as shown in Fig. 1) not flanged but welded on. Before assembly, the resonator was chemically polished and then anodized (≈400 Å).

The second helix resonator (Helix II) had a helix of 8.0 x 1.0 mm Nb tubing, welded into the same outer tank. The lower cover of the outer tank was flanged. Before measurement the resonator was electropolished and anodized (≈400 Å).

Table I shows some data on both helix resonators gathered together. The following abbreviations have been used: f = resonant frequency, G = geometric factor, H_p = maximum magnetic field on the surface, P_c = power loss, Q = quality factor of the resonator, 2a = helix diameter, n = number of turns, s = pitch, Δf = static frequency shift.

<u>Table I:</u>

Helix I: 2a = 6.4cm; s = 1.0cm; n = 13

f/MHz	80	139,5	195,2	251	305
G/Ω	4,2	4,9	5,4	5,7	6,0
$\frac{H_p[\text{Gauß}]}{\{P_c Q[\text{Watt}]\}^{1/2}}$	0,069	0,063	0,08	0,08	0,08
$\frac{P_c Q[\text{Watt}]}{\Delta f[\text{kHz}]}$	$3,9\times10^5$	$2,4\times10^5$	$2,0\times10^5$	$2,3\times10^5$	$2,3\times10^5$

Helix II: 2a = 6.6cm; s = 1.18cm; n = 11

f/MHz	91,4	160,7	224,9	288,8	352,3	413,6
G/Ω	4,4	5,5	5,9	6,3	7,3	8,2
$\frac{H_p[\text{Gauß}]}{\{P_cQ[\text{Watt}]\}^{1/2}}$	0,069	0,076	0,078	0,08	0,08	0,08
$\frac{P_cQ[\text{Watt}]}{\Delta f[\text{kHz}]}$	$12,4\times10^5$	$5,9\times10^5$	$5,1\times10^5$	$4,6\times10^5$	$4,3\times10^5$	$4,6\times10^5$

As is evident in Table I, measurements were made between 80 and 305 MHz and between 91.4 and 413.6 MHz, respectively. The geometry factor G was determined through measurement of the resonator - Q at room temperature. The maximum field intensity H_p on the helix surface was calculated both with the ring model[10] as well as with a model using conformal mapping.[11] Because of the limited validity of both models, the errors in H_p increase markedly for the higher rf-modes. In addition to the calculations, for Helix I frequency perturbation measurements[9] were also made. The relation between the stored reactive power P_cQ and the static frequency shift Δf was determined experimentally.

The resonator was placed in a cryostat, in which the earth's field was attenuated to <5 mGauss with a cylinder of Cryoperm. With two coils mounted inside the Cryoperm - cylinder, an external steady magnetic field (H_{dc}) can be created at the position of the resonator. A solenoid coil produced a field parallel to the resonator - axis ($H_{dc_\parallel}$), while a deformed Helmholtz arrangement formed a perpendicular field ($H_{dc\perp}$). The homogeneity of $H_{dc_\parallel}$ over the resonator volume was ∿5%. The perpendicular field, however had a parallel component of ∿15% of the perpendicular component in the resonator volume. The external magnetic field H_{dc} was impressed above the Nb critical temperature (T_{cNb} = 9.25 K). For Helix I external fields of both directions were used, up to 6 Gauss, for Helix II, up to 3 Gauss. In the transition to the superconducting state, the field was frozen by the incomplete Meissner effect. In cooling a cylinder in a parallel magnetic field, the cylinder outer surface first becomes superconducting, due to the small demagnetization factor. Inside the cylinder, the field is compressed toward the axis, and can only escape with very pure samples (no pinning). Measurements by Y.A. Rocher and J. Septfonds[12] on Nb-cylinders show that only with very pure samples (residual resistance ratio RRR ≈ 1000) is the flux almost completely displaced. For samples with RRR ≈ 155 to 120, 30% to 60% of the flux is captured. Two Hall probes that we placed in the center of the lower cover and in the middle of the cylindrical part of the outer tank showed that the parallel field $H_{dc_{\parallel}}$ in the neighborhood of the resonator axis suddenly rose (about a factor of 2) at the transition to superconducting, while the perpendicular field $H_{dc\perp}$ didn't show any sudden change. $H_{dc_{\parallel}}$ is compressed toward the axis, while $H_{dc\perp}$ is not noticeably displaced in the freezing-in.

All measurements with imposed external field H_{dc} included a null measurement with H_{dc} = 0. During a measurement sequence, the resonator was warmed no more than ∿50°K. In all cases, the null measurements at the beginning and end of such a measurement sequence agreed well. The Q-value was measured by determining the decay time τ of the stored energy W, $Q = \omega \cdot \tau$. At high rf-field intensities, Q was also determined from the power loss P_c and the static frequency shift $\Delta f \propto W$, $Q \sim \Delta f/P_c$ (see Table I). The added losses caused by the frozen-in flux is described by the added surface resistivity R_H:

$$R_H(H_{dc}) = G\left[\frac{1}{Q(H_{dc})} - \frac{1}{Q(H_{dc}=0)}\right] = R_s(H_{dc}) - R_s(H_{dc}=0) \qquad (1)$$

For determining R_H, the total geometry factor G (Table I) was used, incorrectly. Because of the inhomogeneous distribution of the frozen flux over the surface, a partial geometric factor G_p should be used, one which is dependent on the direction of the superimposed external field. Only for simple resonators, and for certain assumptions concerning the distribution of the frozen-in flux, can the partial geometric factor be calculated. However, in the evaluation of R_H from (1), only the frequency dependence and the absolute value of R_H are in error by $G_p/G = g(f)$. The dependence on temperature and the rf-field intensity and also the relative frequency dependence are independent of the geometry factor G which is used.

III. MEASUREMENT RESULTS

In agreement with other measurements[1-7,11] we have observed that for superimposed external fields ($H_{dc} \leq 6$ Gauss), the added surface resistivity R_H is approximately proportional to H_{dc}.

$$R_H \sim H_{dc} \qquad (2)$$

For Helix II the measured values scatter about an average value by ∿20%, which cannot be explained by measurement error. The cause may be due to different flux-freezing-in at each measurement.

In the following we first describe measurements with small rf-field intensities ($H_p \leq 5$ Gauss), and subsequently measurements are reported concerning the dependence on the rf-field intensity.

a) Small RF-Field Intensity, $H_p \leq 5$ Gauss:

For small rf-field intensities, the added surface resistivity R_H is independent of H_p. In this range, the temperature dependence of R_H between T = 4.2 K ($\hat{=}$ t= T/T_c= 0.455) and T = 1.4 K ($\hat{=}$ t = 0.151) was measured for various rf-modes. In Fig. 2a, b, R_H is plotted against $[1-(T/T_c)^2]^{-1}$. Over the measured temperature range, $R_H(T)$ may be approximated as a straightline function in the chosen representation (Fig. 2a). For Helix II, above roughly T≈3K, the increase of R_H with increasing T becomes somewhat weaker (Fig. 2b). As the graphical representation of $R_H(T)$ shows, $R_H(T)$ may itself be represented as the sum of two terms $R_H(T) = R_H(0) + R_H\ (T/T_c)^2/(1-T/T_c)^2)$. This representation is equivalent to the following, which is chosen to simplify comparisons to other measurements.

$$R_H(T,f) = R_H(0,f)\,\frac{1}{1-(T/T_c)^2}\left[1+r_T(f)\,\left(\frac{T}{T_c}\right)^2\right]$$

$$= \frac{H_{dc}}{H_c(0)}\cdot\frac{R_{NL}}{\gamma(f)}\cdot\frac{1+r_T(f)(T/T_c)^2}{1-(T/T_c)^2} \qquad (3)$$

In this, $H_c(0)$ = 1980 Gauss = critical thermodynamic field at $T = 0$, $R_{NL} = 0.26 \cdot 10^{-3} \cdot \sqrt{f/MHz}\,(\Omega)$ = normal conducting surface resistivity with normal skin effect, $\gamma(f) = \gamma \cdot (\frac{100MHz}{f})^{\alpha}$ and $r_T(f) = r_T \cdot (\frac{100MHz}{f})^{\beta}$ are fitted parameters.

$\gamma(f)$ is modified through the use of the total geometry factor G in (1) rather than the true partial geometric factor G_p. $r_T(f)$ is a relative quantity and hence independent of the geometry factor used. In a helix, $r_T(f)$ is thus also independent of the direction of the imposed external field, as is evident from Fig. 3a, b. From Fig. 3a, b it is further evident that $r_T(f)$ is somewhat different for the two helices. The measured values of $r_T(f)$ and $\gamma(f)$ are presented in Table II.

Table II:

	Helix I		Helix II	
	$H_{dc\parallel}$	$H_{dc\perp}$	$H_{dc\parallel}$	$H_{dc\perp}$
γ	190	230	150	110
α	1,35	0,7	1,3	0,7
r_T	10	10	13	13
β	0,4	0,4	0,7	0,7

To get an impression of the magnitude of the additional surface resistivity R_H for the helix resonator, $R_H(T,f)$ is put in a somewhat clearer form (Fig. 4a, b).

Helix I:

$R_H(T=0,\ H_{dc},f) \approx 0.7\ (10^{-8})H_{dc}/\text{Gauss} \cdot (f/100MHz)^{1.85} [\Omega]$ (4a)

$R_H(T=0,\ H_{dc},f) \approx 0.6\ (10^{-8})H_{dc}/\text{Gauss} \cdot (f/100MHz)^{1.2} [\Omega]$ (4b)

Helix II:

$$R_H(T = 0, H_{dc}, f) \approx 0.9(10^{-8}) H_{dc}/\text{Gauss} \cdot (f/100\text{MHz})^{1.8} \ [\Omega] \quad (4c)$$

$$R_H(T = 0, H_{dc}, f) = 1.2(10^{-8}) H_{dc}/\text{Gauss} \cdot (f/100\text{MHz})^{1.2} \ [\Omega] \quad (4d)$$

In Fig. 4 a, b the measured values of $R_H(f)$ are shown for an imposed external field of $H_{dc} = 1$ Gauss. The measurement points are averages of several measurements with external fields $H_{dc} \leq 6$ Gauss. At 4.2 K, $R_H(T,f)$ increases less rapidly with increasing frequency than at 1.5 K. In Eq. (3) both of the terms are considered through the differing f-dependency.

b) R_H as a Function of the RF - Field Intensity H_p

For small rf-field intensity ($H_p \leq 5$ Gauss), R_H is independent of H_p. With increasing rf-field intensity, we observe a monotonic increase in R_H, e.g., for T = 1.4 K and f = 91.4 MHz, for $H_p = 500$ Gauss, R_H is about 8 times larger than for $H_p \leq 5$ Gauss. For lower frequencies and lower temperatures, the relative increase is greater than at higher frequencies and temperatures. In Fig. 5 is a representation of the added surface resistivity $R_H(H_p)$ as a function of H_p with T and H_{dc} as parameters. Fig. 6a, b shows the total surface resistivity R_s with frozen-in field H_{dc} and the corresponding null-measurement ($H_{dc} = 0$) for f = 91.4 MHz. Corresponding to Eq. (1), R_H is the difference between both curves. The curve of $R_H(H_p)$ may be analytically expressed as the sum of two terms somewhat as in the following form:

$$R_H(H_p, T, f) = R_H(0, T, f)\left[1 + r_H(T,f)\left(\frac{H_p}{H_c(0)}\right)^{\delta}\right] \quad (5)$$

with $\delta = 1$ for $H_p \leq 100$ Gauss for Helix II

and $H_p \leq 15$ Gauss for Helix I

$0.5 \leq \delta < 1$ for $H_p > 100$ Gauss (Helix II) or $H_p > 15$ Gauss (Helix I)

$R_H(0,T,f)$ is the H_{dc} - proportional added surface resistivity for small rf-field intensity (Eq. 3). $r_H(T,f)$ is shown in Fig. 7. r_H is somewhat independent of the direction of the imposed external field. It is, however, somewhat different in both resonators. For higher frequencies $r_H(T,f)$ decreases, $r_H(T,f) \sim 1/f^{1-2}$. The decrease of $r_H(T,f)$ with increasing frequency means that the relative increase of $R_H(H_p)$ at higher frequencies becomes less. In addition, $r_H(T,f)$ is about 2 to 3 times smaller at 4.2 K than at 1.4K. The curve of $R_H(H_p)$ differs in the two measured helix resonators respecting the increase with H_p. For the exponents δ in Eq. 5, we have, for rf-field intensities H_p up to $\sim$500 Gauss in the fundamental modes of both resonators, evaluated the following values:

	Helix I f_o = 80 MHz	Helix II f_o = 91,4 MHz
T	δ	δ
1,4 K	0,7 - 0,85	0,6 - 0,9
4,2 K	1	0,5

The agreement of both resonators at 1.4 K is quite good, at 4.2 K, however, the deviation in the curve of $R_H(H_p)$ is considerable. For Helix II, $R_H(H_p)$ was also measured at 288 MHz up to high field intensities. As in the case of 91.4 MHz, $\delta \simeq 0.6 - 0.85$ at 1.4 K. For higher external fields H_{dc}, at the most δ decreases slowly.

IV. DISCUSSION

We first give results of measurements on Nb-resonators in the GHz - range[4] and on helix resonators out of pure tin[5] in the 100 MHz - range. P. Kneisel and O. Stoltz[4] studied the influence of frozen-in magnetic flux on resonators of pure Nb for the 2 to 5 GHz range, in the temperature - range of $t = T/T_c = 0.455$ to $t = 0.15$. The observed added surface resistivity R_H was found to be, as in the case of lead[1,2], well fitted by

$$R_H = \frac{H_{dc}}{H_c(0)} \cdot \frac{R_{NL}}{\gamma} \frac{1}{1-t^2} \tag{6a}$$

with $\gamma \simeq 1$. Within the bounds of the measuring accuracy, it was observed as in Ref. 3 that there was no change in R_H with increasing rf-field intensity. J.M. Victor and W. H. Hartwig[5] reported on measurements on tin ($T_c = 3.72$ K; $H_c(0) = 306$ Gauss) between 60 and 350 MHz.

The measurements were made at small rf-field intensities ($\sim$1 Gauss), with temperature range from $t = 0.5$ to $t = 0.89$. In this temperature range, the observed added surface resistivity R_H was described by

$$R_H = \frac{H_{dc}}{H_c(0)} \cdot \frac{R_{NL}}{\gamma} \left[(1-t^2)(1-t^4)^{1/2}\right]^{-1} \tag{6b}$$

For reduced temperatures $t < 0.5$ the temperature dependence of (6b) is practically the same as that of (6a). The frequency dependence of R_H was not accurately investigated in Ref. 5. From the measured values one gets a γ-value of about 15.

The results in the GHz-range, as well as the results for small rf-field intensities in the 100 MHz-range for tin may be described by a simple model.[1,2]

The core of a flux-tube is considered to be normally conducting. The rf-current passes through these normal regions. The increased losses from the frozen-in field are proportional to the normal area. Since the flux quantum ϕ_0 doesn't change in value, the area A of a flux tube must so change with temperature, that $\mu \cdot H_{core} \cdot A = \phi_0$ remains constant. With the assumption that $H_{core}(t) = H_c(t) = H_c(0)\cdot(1-t^2)$, it follows that $A \sim (1-t^2)^{-1}$. For a frozen-in field H_{dc}, the fraction of normal surface to the total surface is approximately given by H_{dc}/H_c. For the measurements on Pb, as well as those on Nb in the GHz-range, it was observed that $R_H \sim \omega^{0.5-0.67}$; relative to the frequency dependency; it behaves like the normal surface resistivity R_{NL} which includes normal conduction and anomalous skin effect. The penetration depth of the rf-field in the flux tube must then be given approximately by the skin depth δ_{sk}. Only when the diameter of a flux tube is large relative to δ_{sk}, can the rf-field penetrate as far as the skin depth. Otherwise, the penetration depth of the rf-field into the flux tube is determined by the smaller superconducting penetration depth λ ($\lambda \approx 500$ Å). To explain the observed frequency dependence of R_H, Ref. 1 assumed that for lead (Type I superconductor), several flux quanta form a flux tube with a diameter large relative to δ_{sk}.

For Nb (Type II superconductor), having several flux quanta in one flux tube is energetically unfavorable. Because of the "unterschwingens" of the magnetic field[13], however, the flux tubes in Nb attract and can form a flux tube cluster whose diameter is large relative to the skin depth. Relative to the penetration of the rf-field, a flux tube cluster behaves similar to a normal region of the same size. According to this model, the normal flux tube core would give a relation for the added surface resistivity R_H like that given in (6a). Gilchrist and Monceau[14] consider the added surface resistivity in the mixed state (above H_{c1}) at higher frequencies (to GHz) as flux-flow resistance of the oscillating flux quanta. By neglecting pinning forces one can calculate, for small rf-field intensity, the resistance as:

$$R_H = R_{NL} \cdot \sqrt{\frac{B_{dc} \cdot \rho_f}{H(B) \cdot \rho_{NL}}} \approx R_{NL} \sqrt{\frac{B_{dc}^2}{H(B) \cdot H_{c2}}}$$

For the flux-flow resistance ρ_f the relation given by Kim et al.[14] was used. If one considers that for small B, then $H(B) \approx H_{c1}$ and that $\sqrt{H_{c1} \cdot H_{c2}} \sim H_c$ applies, one gets for R_H the same relation (6a) as for the model of normal cores. Measurements in the GHz-range for Pb and Np are satisfactorily described by both models.

Our measurements on Nb in the 100-MHz range deviate therefrom, and, indeed, both regarding the temperature and the field strength dependence. The strong T-dependence at small rf-field strengths can possibly be related to the deep-lying state in the gap. In pure materials (mean free path greater than the coherence length $\xi_{Nb} \approx 400$ Å),the deep-lying states in the energy gap in a flux tube are given by Δ^2/E_F (Δ = Gapparameter; E_F = Fermienergy)[16]. For Nb, this is about 30 MHz. For stationary flux tubes and at frequencies comparable to the interval of the conditions in the flux tube, the deviations in comparing to the model of quasinormal cores or to the flux-flow model are not so very surprising. A cause for the increase of added surface resistivity with rf-field strength (Eq. 5, Fig. 5,6) can be connected to the motion of the flux tube under the influence of the Lorentz-force.[17,18] Among other things, losses which are caused by pinning forces (hysteresis losses) can lead to field-intensity-dependent surface resistivity.

At low frequencies ($f \lesssim 10$ kHz), the influence of frozen-in flux ($H_{dc} \lesssim 10$ Gauss) on the A. C. losses of Nb-samples has been studied[12,19]. For the surface resistivity, measured values could be approximately represented as $R_H \sim f \cdot H_{ac}^{\alpha}$ with $\alpha \approx 0.5 - 1.5$, where f = frequency and H_{ac} = amplitude of the A.C. field. Melville[20] has proposed a model in which frozen-in flux tubes perpendicular to the surface undergo a bending motion under influence of the Lorentz forces, $K_L = 1/c\ j_{ac} \cdot \phi_0$. The pinning force p(x), which opposes any motion, gives rise to hysteresis losses. For the loss P_{Hyst} per unit surface, Melville derives the following value:

$$P_{Hyst} = \frac{2}{3} \frac{H_{dc}}{H_{c1}} \cdot \frac{H_{ac}^3}{I_c} \cdot f \Rightarrow R_H = \frac{2}{3} \frac{H_{dc}}{H_{c1}} \cdot \frac{H_{ac}}{I_c} \cdot f \qquad (8a)$$

H_{c1} = lower critical magnetic field ($H_{c1}(T=0, Nb)$ = 1400 Gauss);
I_c = critical current density is a measure of the pinning behavior in the neighborhood of the surface and is therefore dependent on the material properties. The hysteresis loss L per period, $L = P_{Hyst}/f$, is independent of the frequency, as long as the bending amplitude x_o of a flux tube in the A.C. field depends only on the Lorentz force, i.e., the flux tube distribution comes into equilibrium instantaneously with the A.C. field. For the higher frequencies, i.e., for higher flux tube velocities, in addition to the pinning forces, frictional forces[15], $K_v = \eta \cdot \dot{x}$ (η = viscosity) appear. The motion of a flux tube is qualitatively expressed by .

$$\eta \cdot \dot{x} + p \cdot x = 1/c \; j \; \phi_o$$

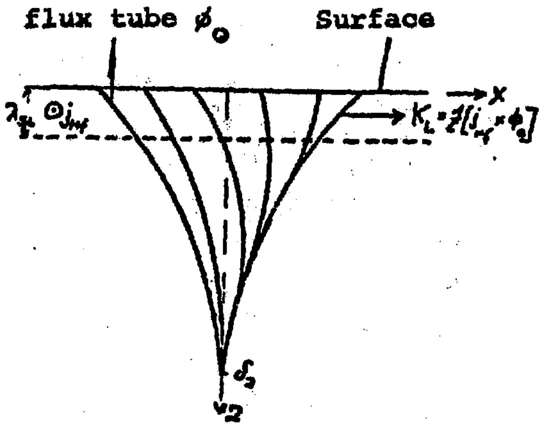

Bending motion of a flux tube perpendicular to the surface under influence of the Lorentz-force - $K_L = \frac{1}{c} [j_{HF} x \phi_o]$

x is the bending excursion, $p \cdot x$ is the linearized pinning force, $j = j_o e^{i\omega t}$ is the rf current ($j_o \sim H_{HF}$). A force which is connected to the elastic tension in the bending of a flux tube and the inertial force[16] ($= m_{\phi_o} \cdot \ddot{x}$) were not considered. With the expression $x = x_o e^{i(\omega t + \delta)}$ one gets for the amplitude x_o:

$$x_o = \frac{1}{\eta \cdot c} \cdot j_o \phi_o \; \frac{1}{\sqrt{\omega^2 + \omega_p^2}}$$

in which the pinning frequency[14,18] $\omega_p = P/\eta$ is that frequency at which the viscous force equals the pinning force. For low frequencies, $\omega \ll \omega_p$, x_o is independent of frequency, i.e., in equilibrium with the A.C. field. For frequencies $\omega > \omega_p$, x_o decreases approximately inversely proportional to the frequency. $1/\omega_p$ is the relaxation time for the motion of flux tubes in the neighborhood of the surface. The hysteresis loss L per period is proportional to the area swept over ($\simeq x_o \cdot \delta_z \sim x_o^2$), proportional, $L \sim x_o^2 \sim 1/f^2$ for $f \gg f_p$.

For frequencies greater than the pinning frequency, the hysteresis loss $P_{Hyst} = L \cdot f \sim 1/f$ should therefore be inversely proportional to f.

For the surface resistivity, which is connected to the hysteresis loss through the bending motion, one gets approximately:

$$R_H(f) \sim \frac{H_{dc}}{H_{c1}} \cdot \frac{H_{ac}}{I_c} \frac{f}{1+(f/f_p)^2} \tag{8b}$$

For low frequencies ($f \ll f_p$) Eq. (8a) and (8b) are identical. Above $f \sim f_p$ the hysteresis losses decrease with increasing frequency.

The field-intensity dependent term of R_H (Eq. 5) has been qualitatively described through pinning losses (Eq. 8b) relative to both frequency dependence and field strength dependence.

Finally, we compare the measurement results at low frequencies[12,19] with our measurements, on the basis of the model of pinning losses through bending motion.

From the measurements of J. C. Male[19] at $f \leq 400$ Hz, $T \simeq 4.2$ K, one gets[20] for the hysteresis loss per period: $L \simeq 2 \cdot 10^{-4}$ Wsec/m^2 at $H_{ac} \simeq 500$ Gauss and $H_{dc} = 200$ Gauss. From this, one gets by extrapolation to $H_{dc} = 1$ Gauss and $f = 1$ kHz a surface resistivity

$R_H(f = 1\ \text{kHz}, H_{dc} = 1\ \text{Gauss}, H_{ac}) \approx 10^{-11} \cdot H_{ac}/H_c(0)\ [\Omega]$. The measurements of Rocher and Septfonds[12] at $f \leq 10$ kHz and $H_{dc} \leq 10$ Gauss yields approximately a surface resistivity

$$R_H(f = 1\ \text{kHz}, H_{dc} = 1\ \text{Gauss}, H_{ac}) \approx 1.6 \cdot 10^{-10} H_{ac}/H_c(0)\ [\Omega].$$

In order to compare these values with ours, we must know the approximate partial geometric factors. From the following considerations, the partial geometric factors for $H_{dc_\parallel}$ and $H_{dc\perp}$, $G_{p_\parallel}$ and $G_{p\perp}$, may be approximately determined. In the fundamental mode, the maximum z-field of our helix approximately equals the maximum r-field.

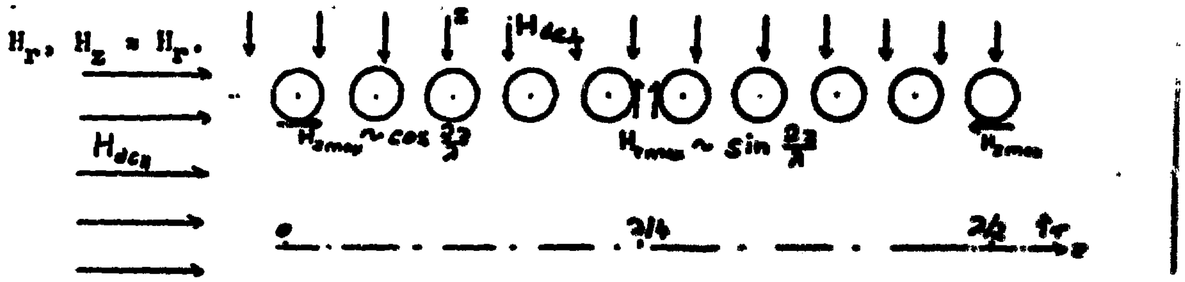

Field Distribution in a Helix. $H_{z_{max}}$, $H_{r_{max}}$ are rf peak magnetic fields on the surfaces.

The parallel or perpendicular frozen-in steady field occur primarily at places where either H_r or H_z-field is. Since the geometric factor is inversely proportional to the surface integral $\int_S H_t^2 df$ [with s=surface, H_t=tangential field] over the effective rf-field, one would expect that the partial geometric factor in the fundamental mode would have a value of approximately 2G, $G_{p_\parallel} \approx G_{p\perp} \approx 2$ G, since about half of the total surface must be integrated over. For the higher modes similar considerations do not work, since $H_{z_{max}} \neq H_{r_{max}}$ and therefore the regions where the flux exits have very different weighting factors (so integral is not simply an area). The partial geometry factors in the higher rf-modes can nevertheless be evaluated if one assumes that for small rf-field intensities and low temperatures, $R_H(T\to0,f)$ is proportional to $R_{NL} \sim \omega^{1/2}$. Such a dependence is to be expected from the model of normally conducting cores and the flux-flow model.

From $R_H(T=0,f)\cdot G_p/G \sim f^{1/2}$ one gets (with Eq. 4a-d) for the partial geometric factors:

$$G_{p\parallel} = 2\cdot G\cdot(f/100\mathrm{MHz})^{-1.3}; \quad G_{p\perp} = 2\cdot G\cdot(f/100\mathrm{MHz})^{-0.7}.$$

The corrected value of the surface resistivity is determined by multiplication by G_p/G. The corrected field-intensity-dependent part $R_2(H_p,f)$ of the surface resistivity (Eq. 5) is written as

$$R_2(H_p,f) = R_H(0,T,f)\cdot r_H(T,f)\cdot\frac{G_p}{G}\cdot\frac{H_p}{H_c(0)} = R_2(f)\cdot\frac{H_p}{H_c(0)}$$

The values of $R_2(f)$ as a function of the frequency f are plotted in Fig. 8. The measurements are referred to $H_{dc} = 1$ Gauss. The solid curve is calculated from Eq. 3b. The pinning frequency $f_p \approx 20$ MHz is so chosen that the surface resistivity in the kHz-range (R_H(1kHz) $= 1.6\cdot10^{-10}\cdot H_p/H_c(0)\,[\Omega]$)[11] as well as the 100 MHz-range are both fitted as well as possible by the pinning model. The pinning model explains the characteristic forms of the observed field-intensity-dependent terms in R_H. The pinning frequency of 20 MHz is relatively high. Gilchrist and Monceau[14] report for Nb samples treated in various ways pinning frequencies between 10^4Hz and 10^8Hz, whereas disturbed samples (of small RRR, high I_c) show higher pinning frequencies.

V. SUMMARY

The added surface resistivity R_H caused by frozen-in magnetic flux in the 100-MHz regions show a complex behavior compared to that in the GHz-range. It is observed to have a stronger temperature-dependence, Eq. (3), and an increase of R_H with increasing rf-field intensity, Eq. (5). The field intensity-dependent term of R_H may be caused by motion of the frozen-in flux tubes in the rf field.

The increase of R_H with increasing rf-field intensity requires that when high rf-field intensities are used, better magnetic shielding be employed than is necessary for measurements with low rf-intensities. For a helix structure (f ≈ 90 MHz operating in an unshielded earth's field (≈0.5 Gauss), the added surface resistivity $R_H(T = 1.4\ K, H_p = 500\ \mathrm{Gauss}) = 2\text{-}3 \cdot 10^{-8}\Omega$, the corresponding quality factor $Q_H = G/R_H$ amounts to about 2 (10^8).

LITERATURE REFERENCES

[1] J. M. Pierce, thesis (Stanford Univ. 1967)

[2] J. Halbritter, K. Hoffman, Proc. of the 1966 Lin. Acc. Conf., Los Alamos, 1966, p. 499

[3] W. Bauer et al., Part. Acce. Conf., San Francisco, März 1973 IEEE Trans NS-20, No. 3 (1973)

[4] B. Piosczyk, P. Kneisel, O. Stoltz, H. Halbritter; Part. Acc. Conf., San Francisco, März 1973 bzw. Interne Notiz Nr. 213, März 1973

[5] C. R. Haden, W. H Hartwig, Phys. Rev. 148, 313 (1966)
J. M. Victor, W. H. Hartwig, J. Appl. Phys. 39, 2539 (1968)
C. R. Haden, W. H. Hartwig, J. M. Victor; IEEE Trans.Magn. Vol. Mag. 2 No. 3, 331 (1966)
W. H. Hartwig, Proc. of IEEE, Vol. 61, No. 1, Jan. 1973, S.58-76

[6] J. E. Vetter et al., Proc. of the 1970 Proton Lin. Acc. Conf., Batavia, p. 249, bzw. Intern Notiz Nr. 118 / 1970

[7] R. Benaroya et al., Appl Phys. Lett. 21, 235 (1972)

[8] Ch. Jones, J. Judish, NAL Oak Ridge, private Mitteilung

[9] J. L. Fricke et al., Part. Acc. 3, 35, 1972
J. L. Fricke et al., Interne Notiz 183 / Mai 1972
A. Citron et al., Proc. Int. High Energy Acc. Conf., CERN,Genf,1971

[10] O. Siart; Dissertation (Universität Frankfurt, 1971)

[11] A. J. Sierk et al., Part. Acc. 2, 149 (1971)

[12] Y. A. Rocher, J. Septfonds, Cryogenics 7, 1967, p. 96

[13] J. Halbritter, Z. Phys. 2, 43, S. 201, 1971

[14] J. Gilchrist, P. Monceau, 1968, Phil Mag. 18, 237-50

[15] Y. B. Kim et al., Phys. Rev. 139, A1163, (1965)

[16] C. Caroli, P. G. Degennes, J. Matricon; Phys. Lett. 9,4,(1964), 307

[17] F. Irie, K. Yamafui, J. Phys. Soc. Japan 23,2,(1966), 255

[18] J. Gittlemann, B. Rosenblum, J. Appl. Phys. 39, 2617, 1968

[19] J. C. Male, Cryogenics 10, 1970, 381

[20] P. H. Melville, Advances in Phys. 21, 1972, 647

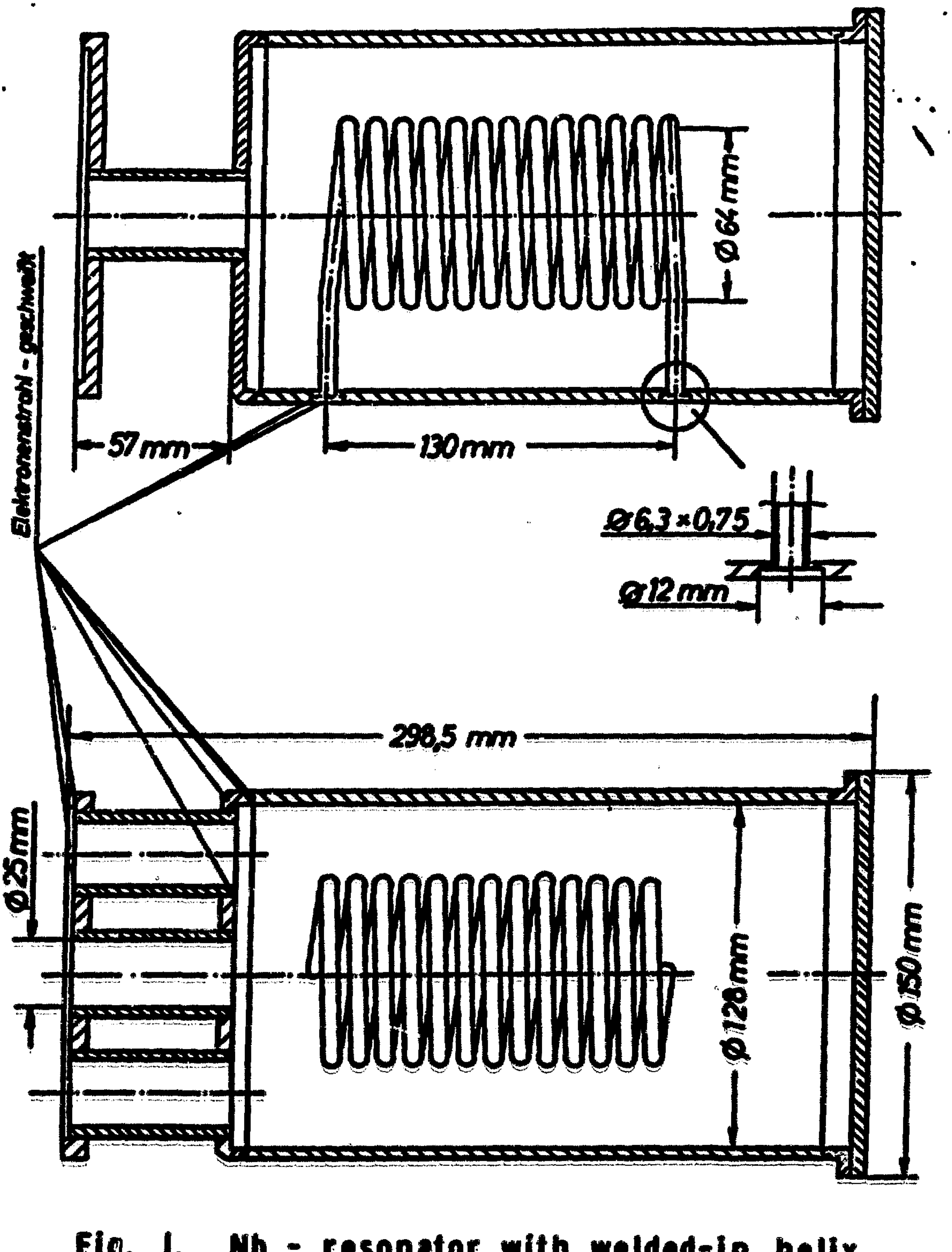

Fig. I. Nb - resonator with welded-in helix

Fig. 2 R_H as a function of temperature in various rf-modes

a) bei Helix I mit $H_{dc_\parallel}$ = 6 Gauß

b) bei HelixII mit $H_{dc_\perp}$ = 1,5 Gauß

a)

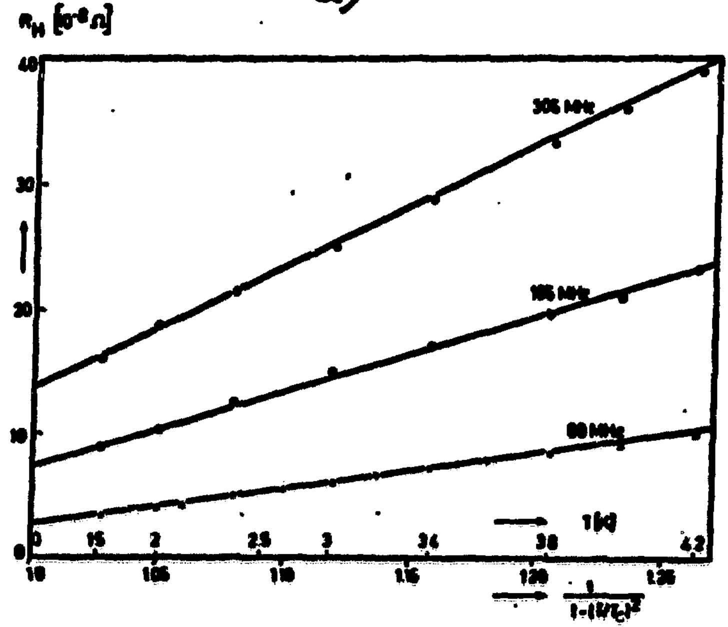

b)

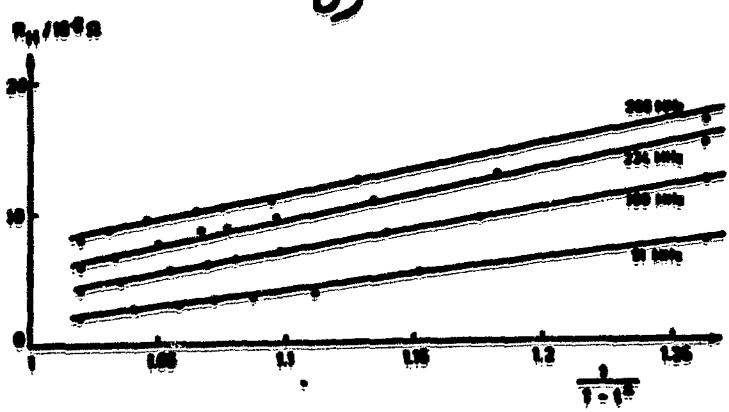

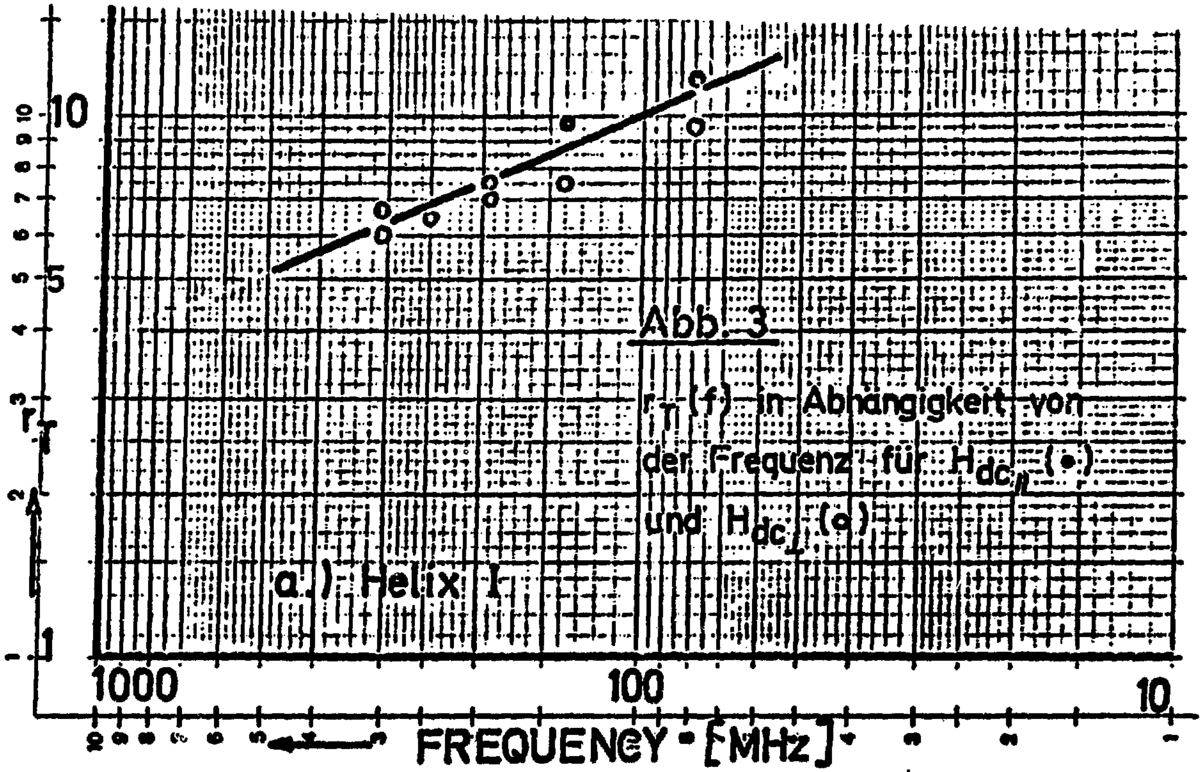

Fig. 3. $r_T(f)$ as a function of frequency for $H_{dc_\parallel}$(o) and $H_{dc\perp}$(o)

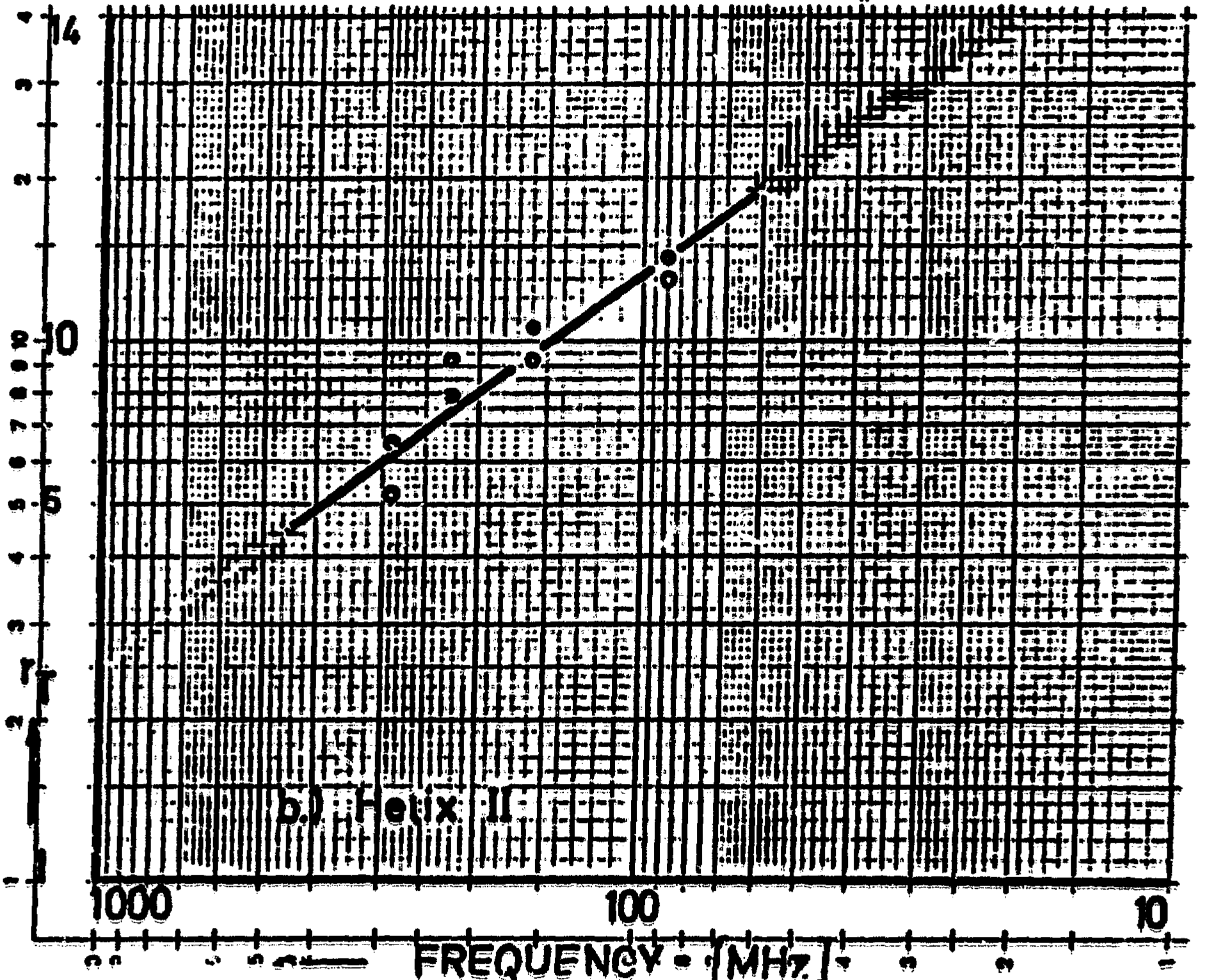

Fig. 4 $R_H(f)$ as a function of frequency f for small rf-field-intensities for T→0 and T = 4.2 K, referred to H_{dc} = 1 Gauss, for parallel (o, •) and perpendicular (senkrechtes) external field (▲, Δ)

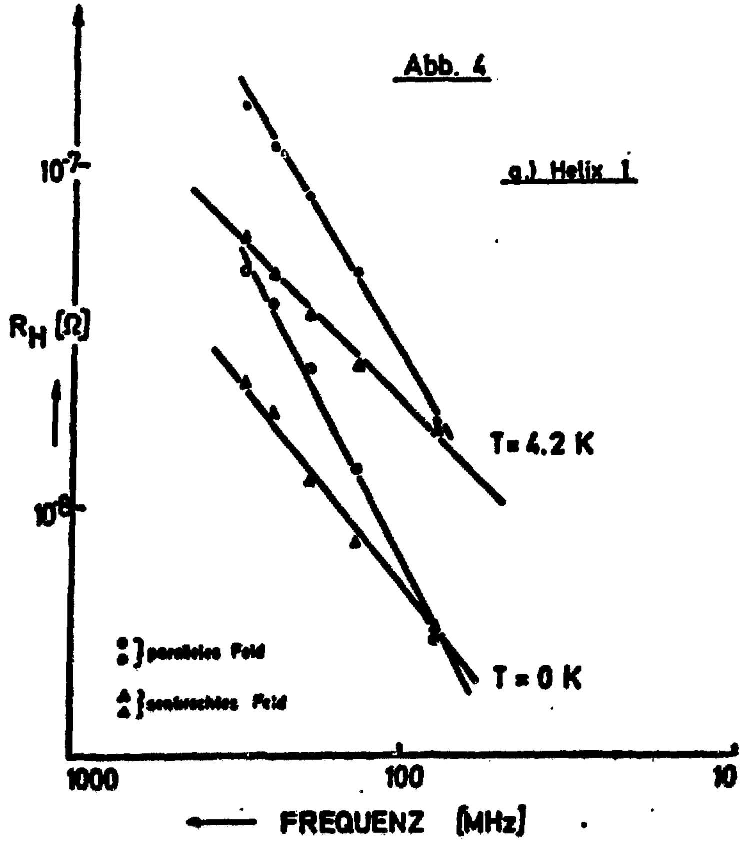

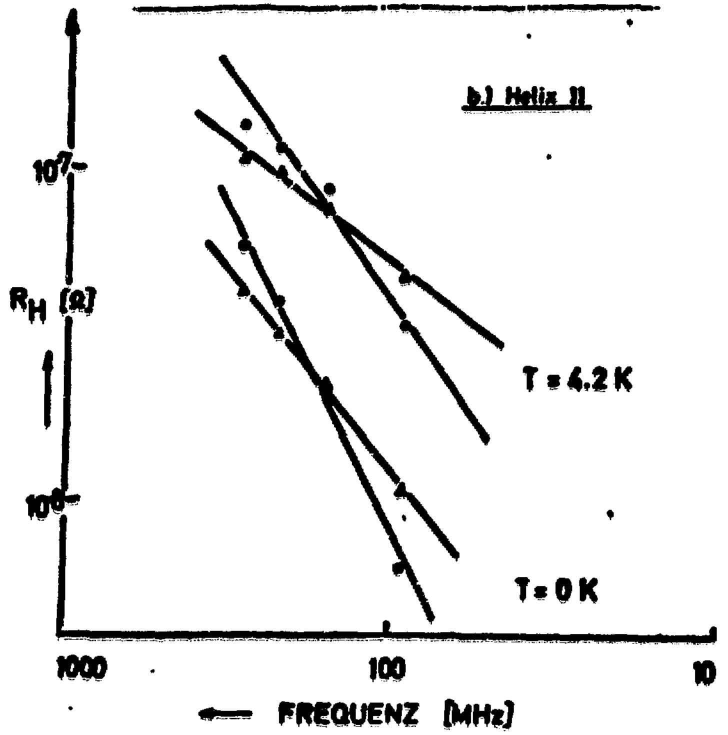

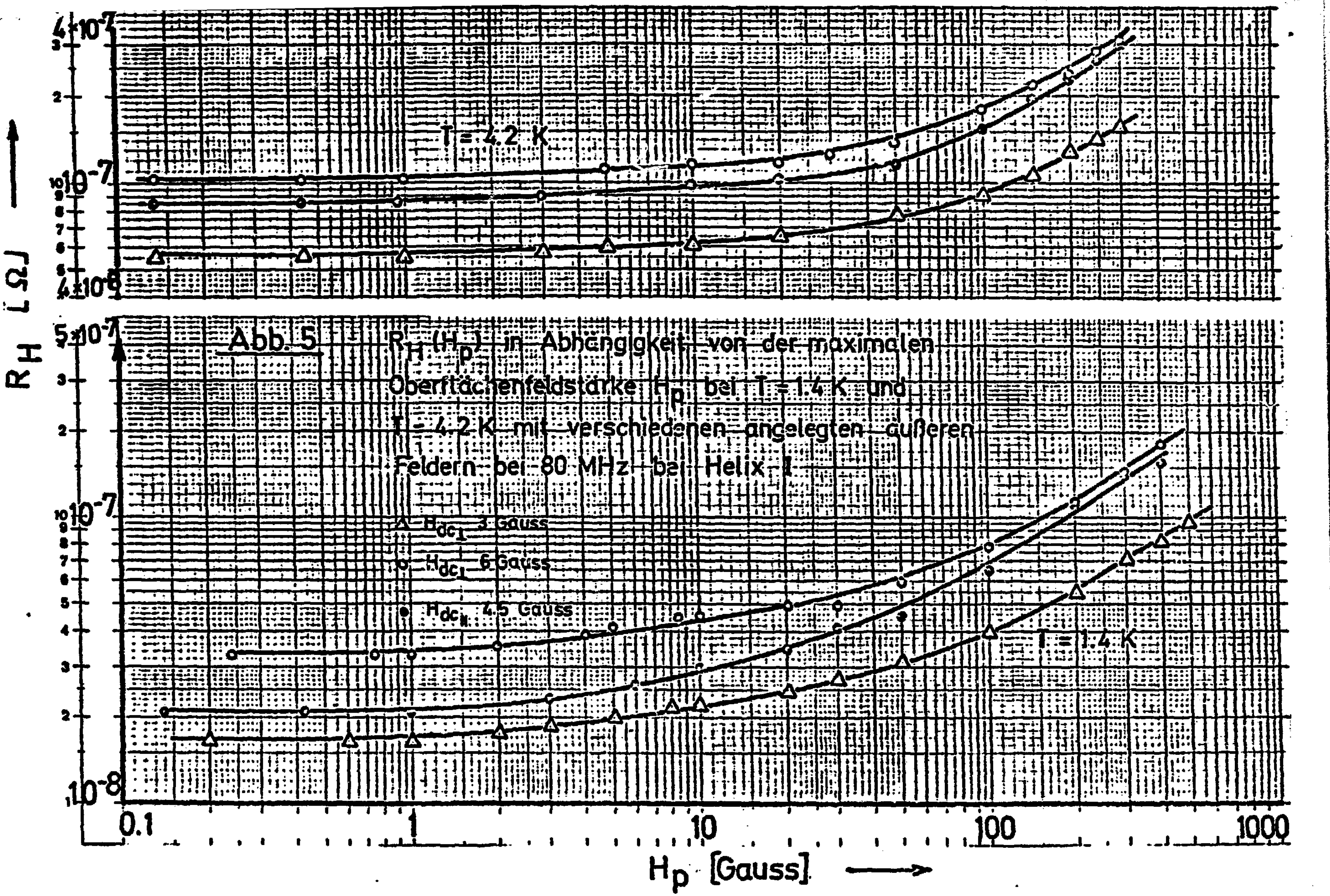

Fig. 5 R_H (H_p) as a function of maximum surface field intensity H_p for T = 1.4 K and T = 4.2 K with various imposed external fields at 80 MHz for Helix I.

Fig. 6 $R_s(H_p)$ as a function of the maximum surface field intensity H_p at T = 1.4 K and 4.2 K for $H_{dc_{\parallel}}$ = 1.5 Gauss and H_{dc} = 0 Gauss for Helix II.

a) at 91.4 MHz

b) at 288 MHz

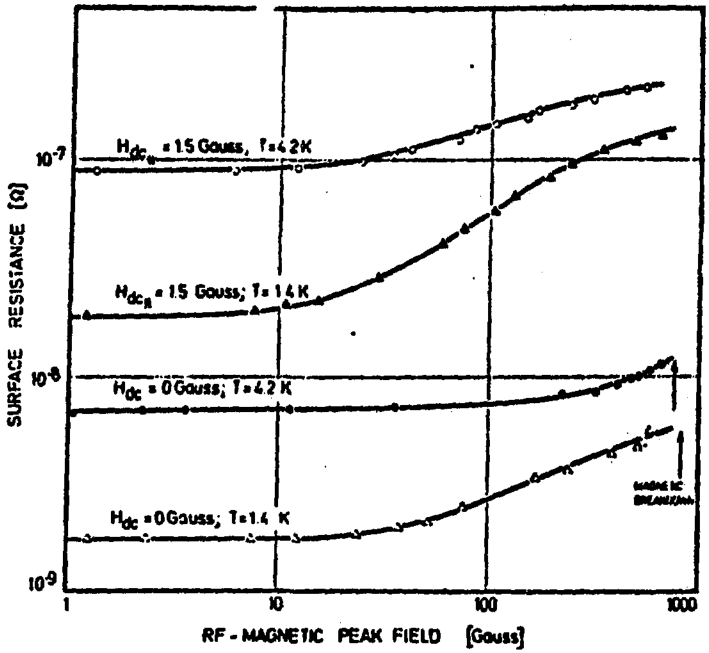

a)

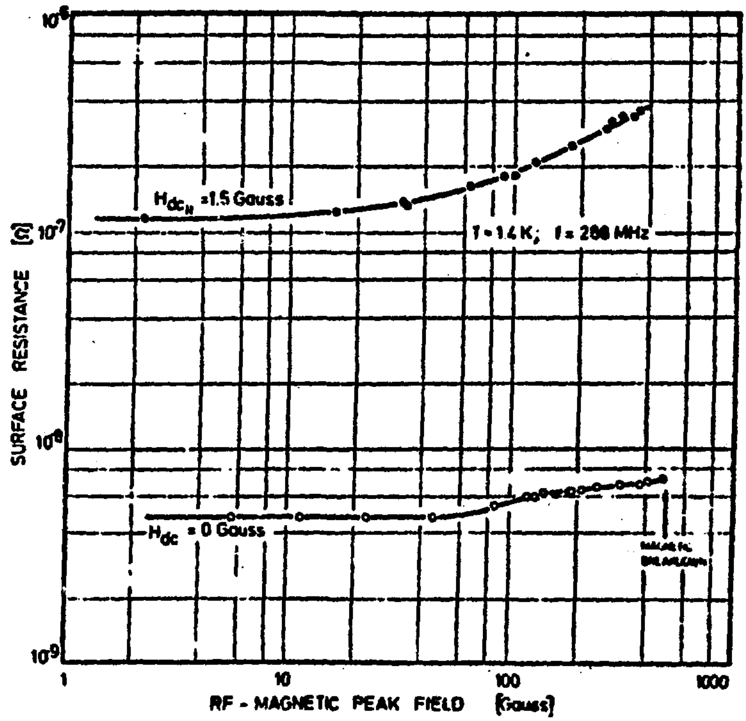

b)

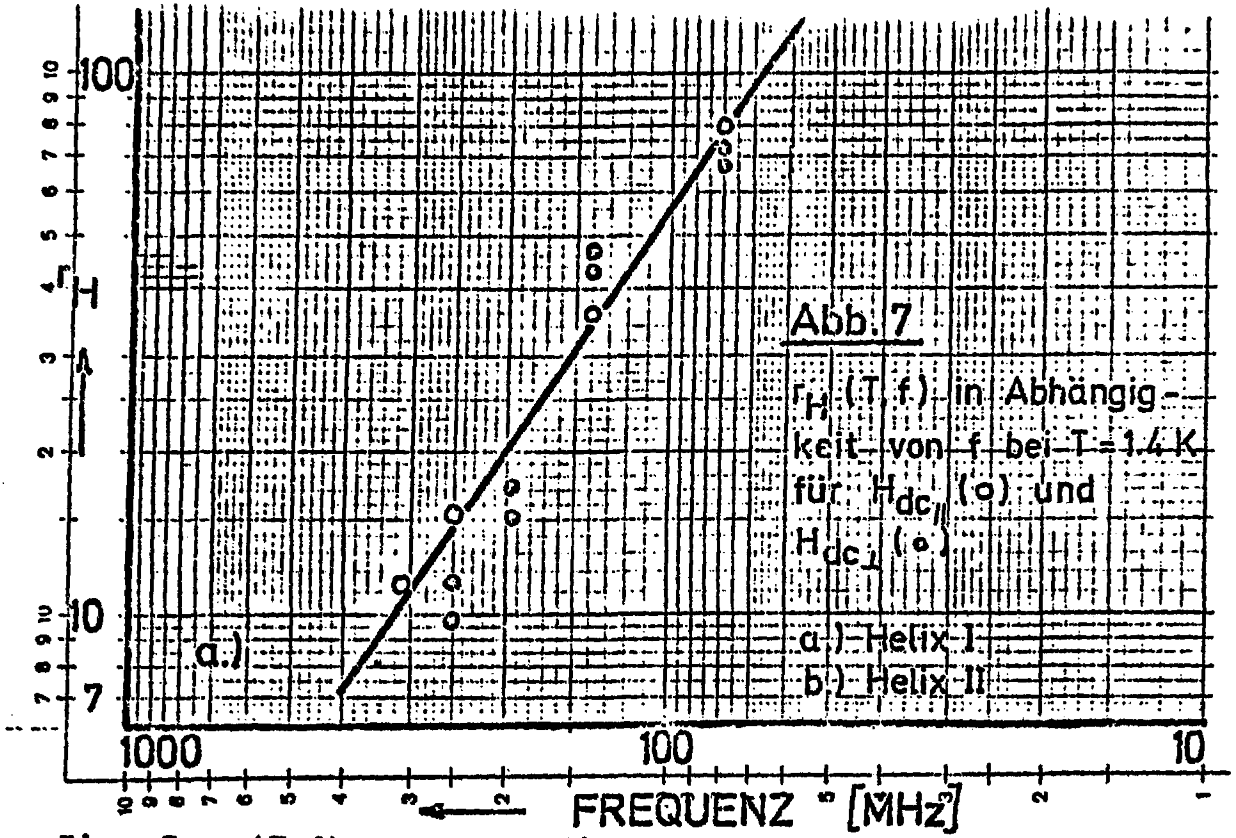

Fig. 7 $r_H(T,f)$ as a function of f for T = 1.4 K for $H_{dc\parallel}$ (o) and $H_{dc\perp}$ (∘)

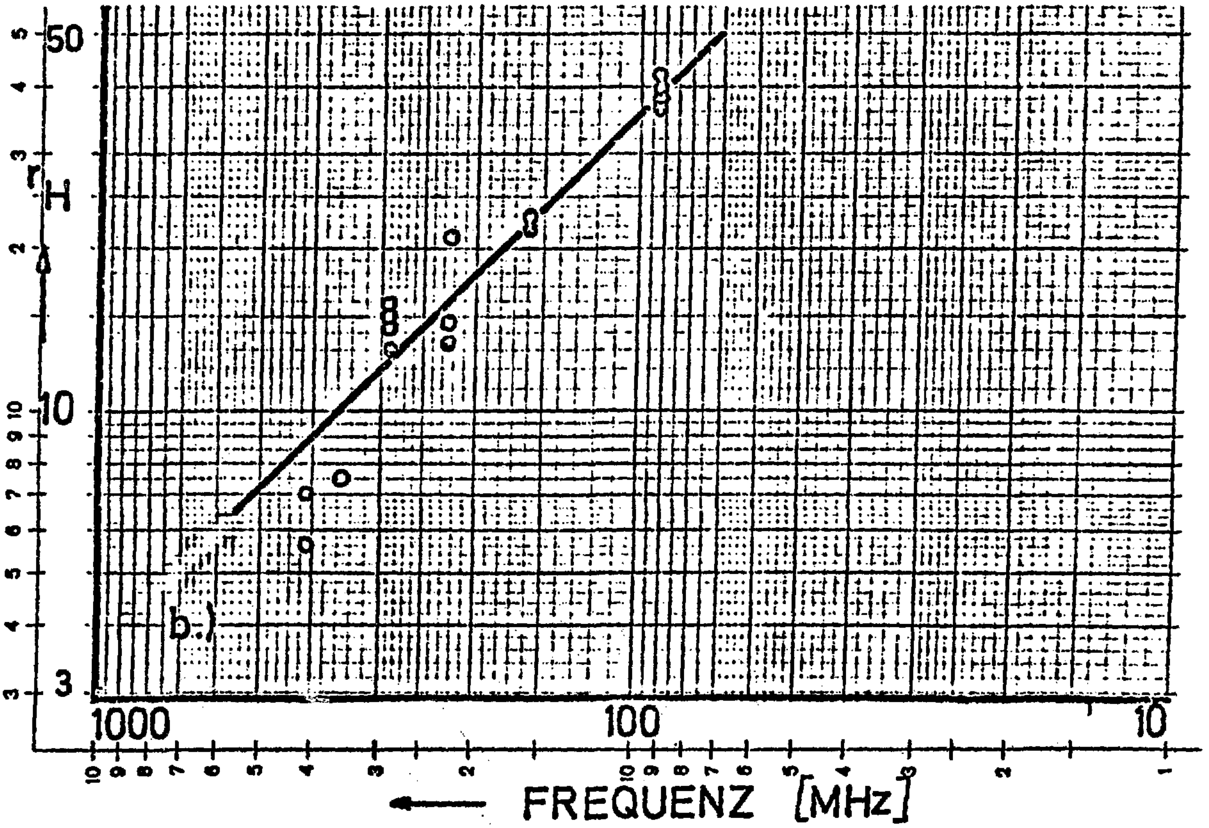

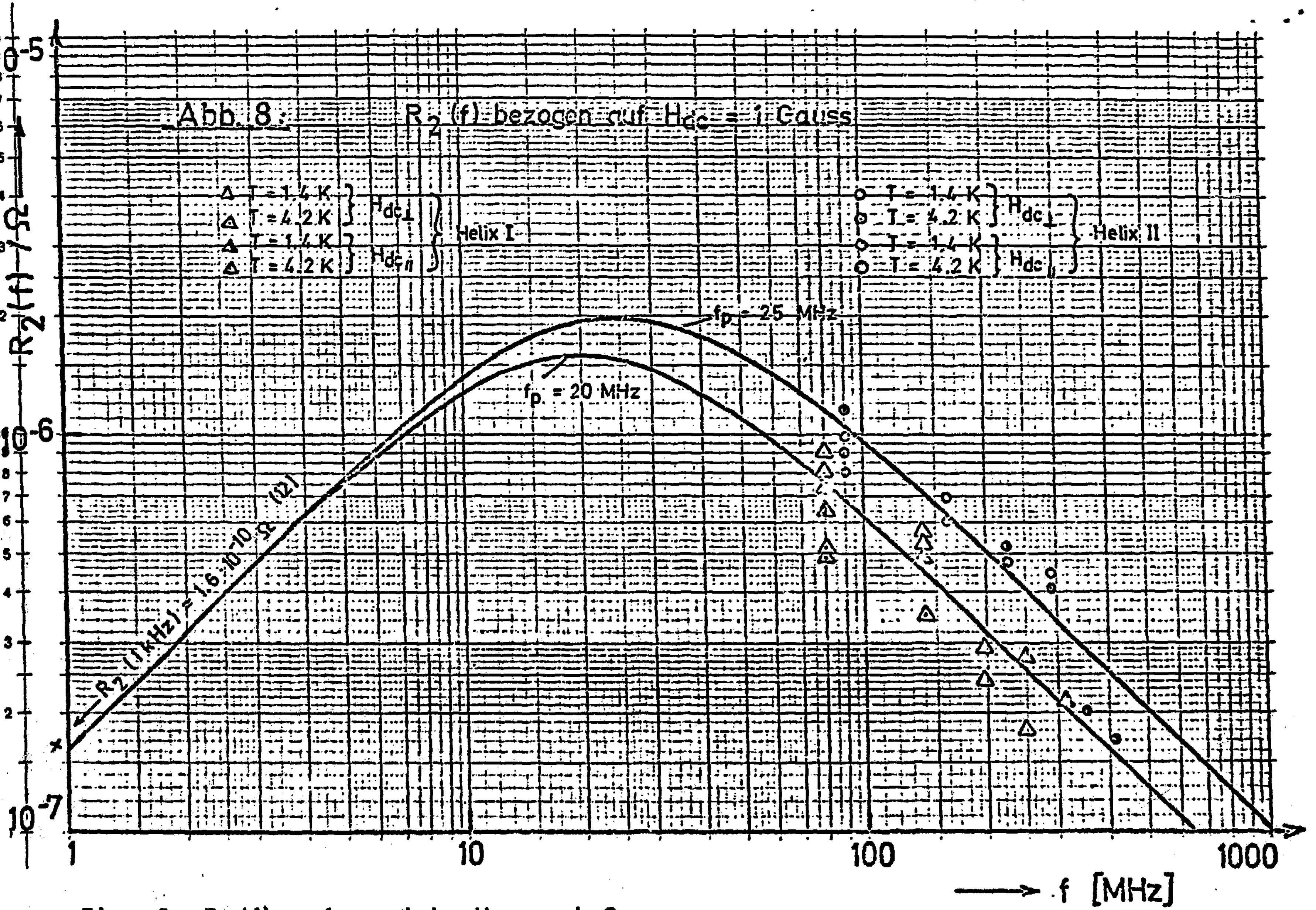

Fig. 8 $R_2(f)$ referred to H_{dc} = 1 Gauss